RSC Advances

PAPER

View Article Online
View Journal | View Issue

Cite this: *RSC Adv.*, 2019, **9**, 25576

Full-color-emitting ($CuInS_2$)ZnS-alloyed core/shell quantum dots with trimethoxysilyl end-capped ligands soluble in an ionic liquid

Huiqing Wang, *[ab] Jiayuan Hu,[a] Min Zhu,[a] Yucheng Li,[a] Hao Qian,[a] Xiaofei Shen,[a] Falk Liebner *[b] and Thomas Rosenau[b]

Received 24th April 2019
Accepted 24th July 2019

DOI: 10.1039/c9ra03066b

rsc.li/rsc-advances

Zinc-copper-indium sulfide (ZCIS)-alloyed quantum dots are emerging as a new family of low toxic I–III–VI semiconductors due to their broad and color-tunable emissions as well as large Stokes shifts. Here, we fabricated a series of ZCIS QDs with tunable PL wavelengths and band-gap energies *via* a facile strategy by varying the ratio of A1–3 stock (Cu^+/In^{3+}) to the B stock (Zn^{2+}) content. The ZnS shell was formed to improve the PL emission efficiency of the core nanoparticles and the PL emission wavelength of the resulting ZCIS/ZnS NCs gradually blue-shifted with an increase in the number of shell layers, resulting in a wide range of emissions from 800 nm to 518 nm that can be tuned by the core compositions or shell layer numbers for ZCIS/ZnS. Finally, the long-chain ligands dodecanethiol/octadecylamine on the quantum dots' surface were efficiently replaced by (3-mercaptopropyl)trimethoxysilane, thus enabling their solubility in an ionic liquid, which was confirmed *via* GC-MS. It also benefited for the co-dissolution of the polymers and chemical binding with other materials through the reactive silanol group, which provide stable and well-distributed ZCIS/ZnS QDs composites or surface coating by the QDs.

Introduction

Semiconductor nanocrystals (mc-NCs) are of great interest for a wide spectrum of applications, such as light emission, photocatalysis,[1] photovoltaics,[2] and biolabeling.[3] Despite their promising optical properties, the intrinsic toxicities of Cd, Hg, and Pb limit their potential in widespread applications. Less toxic materials, which possess similar optical properties, can be found among ternary I–III–VI semiconductors.[4,5] Copper indium disulfide (CIS), for instance, is a direct semiconductor with a band gap of 1.45 eV in the bulk, which closely matches that of the solar spectrum, as well as an absorption coefficient of 10^5 cm^{-1},[6] photostability, biocompatibility, and a relatively long fluorescence decay time. The emission of $CuInS_2$ nanocrystals can be tuned between 950 nm and 500 nm by decreasing the size of the crystallites. However, small particles are less stable and have lower quantum yields than the larger ones. Alloying with other (semiconductive) compounds has recently been described to control the band-gap energy (E_g) and photoluminescence (PL) wavelength of the semiconducting NCs.[7] Thus, another approach is the alloying of $CuInS_2$ with ZnS,[8–10] CdS,[11] $CuGaS_2$,[12,13] and Cu_2SnS_3,[14] among which alloying $CuInS_2$ (E_g = 1.5 eV) with ZnS (E_g = 3.7 eV) is of special interest for very low (~2.2%) lattice mismatch due to their similar crystallographic structures and low toxicity. The band gap of $CuInS_2$–ZnS alloys (ZCIS) can vary between 1.55 and 3.7 eV. Fabricating ZCIS is promising for applications in biolabelling, photocatalysis, solar energy conversion, display technology, and light-emitting diodes. Several literature reports on the direct synthesis of ZCIS NPs have been described.[15–20] Typically, the thermolysis of complexes of dithiocarbamate with Zn^{2+}, Cu^{2+}, and In^{3+} in the presence of oleylamine as an activating agent formed homogeneous nanocrystals.[19] Another approach is a two-step procedure, in which the $CuInS_2$ crystallites are synthesized first and the alloy particles are obtained by cation exchange.[15,21]

Herein, a facile strategy was reported for the synthesis of the ZCIS-alloyed core nanoparticles by varying the ratio of the stock A (Cu^+In^{3+}) to stock B (Zn^{2+}) to rapidly synthesize a series of ZCIS with different compositions using 1-dodecanethiol as the sulfur source and as the ligand. The overcoating of fluorescent mc-NCs with semiconductors of higher band-gap energy is a common way to minimize the non-radiative transitions caused by surface defect trapping to enhance the PL intensity.[22] Here, batch feeding approach was followed for the core growth to deposit a ZnS shell around the ZCIS core NCs with designed layers, which also induced a blue shift as reported and was beneficial in widening the PL range of the ZCIS/ZnS core/shell QDs to provide tunable photoluminescence (PL) emission property.

The ligand covered on the QD surface limited the suitability for further applications.[23] Thus, an effective ligand exchange

[a]*Department of Polymer Science and Engineering, School of Chemistry and Chemical Engineering, Hefei University of Technology, Anhui 230009, China. E-mail: huiqing.wang@hfut.edu.cn; 2604363550@qq.com; 1518814521@qq.com; 1192747003@qq.com*
[b]*Division of Chemistry of Renewables, Department of Chemistry, University of Natural Resources and Life Sciences, Tulln 3430, Austria. E-mail: falk.liebner@boku.ac.at*

was needed to transfer the QDs to the target solvent for their application. The ZCIS QDs obtained by colloidal synthesis at high temperature are usually covered by long-chain ligands, for example, the ligands replaced by mercaptohexanol[24] enabled the solubility in methanol, ethanol, and dimethylformamide, and the ligands exchanged with lipoproic acid,[25] poly(maleic anhydride-*alt*-1-octadecene),[26] or dihydrolipoic acid[27] render the particles water-soluble.[28,29]

Herein, we successfully exchanged the ligand 1-dodecanethiol by 3-mercaptopropyl-trimethoxysilane with the help of the ionic liquid 1-hexyl-3-methylimidazolium chloride as the new solvent. The 3-mercaptopropyl-trimethoxysilane (MPTMS) contains bi-functional groups that can bind to glass surfaces or metal oxide films and polymers *via* hydrogen bonds and covalent bonds. 3-Mercaptopropyltrimethoxysilane had been applied to encapsulate gold nanoparticles,[30] sliver nanoparticles,[31] and so on. Herein, for the first time, it has been applied to encapsulate ZCIS QDs. Further, here the ligand exchange reaction with 3-mercaptopropyl-trimethoxysilane also provide the QDs solubility in the ionic liquid, which is called as a super solvent for many materials and natural polymers such as cellulose,[32–34] collagen[35] keratin,[36] and chitin,[37] which are not soluble in common organic solvents but can be dissolved in ionic liquid; some synthetic polymers are also soluble in the ionic liquid.[38] Therefore, here the MPS–ZCIS/ZnSQDs were applied in homogeneous QD polymer composites or stable surface coating by QDs on other matrices.

Experimental section

Chemicals

Copper(I) iodide (CuI, 99.99%), indium(III) acetate ($In(OAc)_3$, 99.99%), zinc(II) acetate ($Zn(OAc)_2$, 99.99%), 1-dodecanethiol (99.9%), 1-octadecylamine (97%), 1-octadecene (90%), and γ-(mercaptopropyl)trimethoxysilane (95%) were purchased from Sigma-Aldrich Corp. (USA) and used without further purification.

Stock solution series A1–3. The starting materials included the following: (0.05 M Cu^+; Cu : In ratios of 1 : 1, 1 : 2, and 1 : 4); 0.095 g (0.5 mmol) of CuI, 0.292 g (1 mmol) of $In(OAc)_3$, 2.5 mL of 1-mercapto-*n*-dodecane, and 7.5 mL of 1-octadecene. These were placed in a pre-dried three-necked round-bottom flask and degassed under vacuum at 80 °C for 60 min. The mixture was then heated to 160 °C in an argon atmosphere and held at this temperature for about 30 min until a clear green solution was formed. The resulting CuIn stock solution A2 (0.05 M, Cu/In ratio of 1 : 2) was stored at 50 °C under the argon atmosphere until further processing.

Stock solution 2. (0.05 M Zn^{2+}): 0.0918 g (0.5 mmol) $Zn(OAc)_2$, 0.5799 g (2 mmol) 1-octadecylamine, and 9.8 mL 1-octadecene were treated as described above to obtain a colorless solution.

Preparation of ZnCuInS (ZCIS) core nanoparticles

In a typical procedure, 1.0 mL of the stock solution A1 (0.05 mmol Cu^+I^{3+}), 0.7 mL of the stock solution B (0.035 mmol Zn^{2+}), and 1 mL dodecanethiol were mixed in 8.0 mL of ODE in a 50 mL three-necked round bottom flask. This was subjected to three cycles of degassing and purging with argon on a Schlenk line, and then heated to 230 °C in an argon atmosphere under vigorous stirring. The aliquots of each batch were taken at different time intervals and injected into cold toluene to terminate the growth of NCs and to record their optical spectra. When the ideal fluorescent properties were achieved, the mixture was cooled in an ice water bath with stirring and 10 mL of toluene was added to dilute it thereafter. The resulting ZCIS NCs (2 mL) were pipetted into 15 mL centrifuge tubes, precipitated with 8 mL acetone, and then isolated by centrifugation and decantation. The mc-NCs were further purified by repeatedly dispersing the material in toluene and precipitating it in ethanol and acetone. The purified NCs were redispersed in toluene for the optical and morphological measurements or dried in vacuum for XRD measurements.

A series of ZCIS core nanoparticles were prepared with the stock solutions A1–3 and B with Zn^{2+} : Cu^+ in the mole ratios of 1, 0.7, 0.5, 0.25, and 0 at the reaction temperatures of 210 °C, 230 °C, and 250 °C with 0.25–3 mL of DDT.

ZCIS/CIS "core"–ZnS "shell" nanoparticles. The CIS or ZCIS core particles were grown at 230 °C for 60 min as described above. After raising the temperature to 240 °C, the deposition of ZnS on the surface of respective core templates was accomplished by the portion-wise addition of 0.4 mL Zn stock solution, which was injected into the reaction mixture in 5 batches at intervals of 30 min each. The stock A CIS solution can still contain enough sulfur precursor, so the addition of sulfur is not always necessary.[39]

To monitor the reaction, the aliquots were taken before injecting a new batch of Zn stock and their corresponding optical spectra were recorded accordingly. The purification method of ZCIS/ZnS NCs was similar to that of ZCIS NCs.

Solubilization of ZCIS/ZnS nanoparticles in ionic liquids by ligand exchange with γ-(mercaptopropyl)trimethoxysilane. A solution of 0.05 mL γ-(mercaptopropyl)trimethoxysilane in 5.0 mL 1-hexyl-3-methylimidazolium chloride was added to a 5.0 mL solution of ZCIS/ZnS core/shell nanoparticles solubilized in toluene by the lipophilic 1-dodecanethiol ligands. The resulting two-phase system was vigorously stirred at ambient temperature for 30 min, whereupon the mc-NCs moved from the supernatant toluene into the lower ionic liquid phase. The supernatant toluene was separated out for GC-MS detection to confirm the ligand exchange and the ionic liquid phase containing the mc-NCs was collected and stored in cool and dry conditions.

Characterization

For optical analysis, the as-prepared solutions were diluted with toluene to an optical density of approximately 0.1–0.2. The absorption spectra of the ZCIS-alloyed core and ZCIS/ZnS core/shell QDs were collected *via* UV-visible absorption spectroscopy (Lambda 35, PerkinElmer spectrometer). PL emission spectra were recorded using a fluorescence spectrometer (LS55, PerkinElmer, USA). The PL QYs of the QDs dispersed in chloroform

were measured by comparing their integrated emissions with those of a rhodamine 6G (QY of 96%) ethanol standard with an identical optical density of 0.05. X-ray diffraction (XRD, PW1710, Philips Co.) and transmission electron microscopy (TEM) (JEOL JEM-1400) were used for the morphological and structural analyses. For TEM, the NCs were deposited from the dilute toluene solutions onto copper grids with carbon supports by slowly evaporating the solvent in air at room temperature, followed by a second carbon film coating. AFM experiments were performed using a Nanoscope III AFM (Digital Instruments, Santa Barbara, CA) fitted with a 15 × 15 μm scanner. Silicon nitride tips (Digital Instruments) with a spring constant of 0.06 N m^{-1} and a nominal radius of 5–40 nm were used; the images were recorded in both the height and amplitude modes.

The ligand exchange behavior was analyzed by GC-MS (Agilent 5975B inert Series GC/MS System) using 500 μg Br-decane in 250 μL toluene solution as the internal standard. The original ligand 1-dodecanethiol was dispersed again from the QDs into the toluene after the ligand exchange and different concentrations of the decanted toluene were collected for measurement; the amount of ligand exchange was detected by GC-MS as an indirect confirmation of the ligand exchange behavior.

Results and discussion

The ZCIS NCs were prepared in 1-octadecene using In and Zn acetates and copper iodide as the cationic precursors in the presence of 1-amino-*n*-octadecane and 1-dodecanethiol without sulfur injection; 1-dodecanethiol served as the sulfur source. This simultaneously stabilized the resulting NCs.[40] The PL properties (PL peak position and PL intensity) of the resulting ZCIS NCs were strongly dependent on the experimental variables, such as Zn content, Cu : In ratio, 1-dodecanethiol concentration, and reaction temperature. Since the PL QYs of all the as-prepared ZCIS NCs under different experimental conditions were not high (usually less than 5%) and could not approach the desired value for practical applications, the PL QYs were not considered as an experimental variable. The PL QYs were mainly improved *via* the construction of ZnS shells around the ZCIS core nanoparticles, as discussed below. Hereafter, we only describe the dependence of PL wavelength on the experimental variables.

Effect of Zn content

We attempted to tune the PL wavelength of the resulting ZCIS NCs by controlling the Zn : Cu : In ratio while keeping the other experimental variables constant. Different Zn : Cu : In ratios were achieved by controlling the concentration of the precursors during synthesis. Herein, the molar ratio of Zn^{2+} to Cu^{+} in the precursor solution was varied from 0 : 1 to 1 : 1, and equimolar concentrations of Cu^{+} and In^{3+} were used in each case. The color of the quantum dot suspensions in toluene changed from light to dark, as observed in daylight with the increase in reaction time, as shown in Fig. 1A.

Fig. 1A shows that for a reaction time of 90 min, the color of the QD suspension in toluene changes from brownish (λ_{em} = 685 nm; Cu : In : Zn = 1 : 1 : 0) to reddish (λ_{em} = 628 nm; Cu : In : Zn = 1 : 1 : 0.2), orange (λ_{em} = 596 nm; Cu : In : Zn = 1 : 1 : 0.5), yellow (λ_{em} = 575 nm; Cu : In : Zn = 1 : 1 : 0.7), and faint yellow (λ_{em} = 555 nm; Cu : In : Zn = 1 : 1 : 1) with the increasing amount of Zn in the composition. The evident blue-shift in the PL emission wavelengths of the NCs results from an increase in the band-gap energies with the increase in the Zn content. This is ascribed to the incorporation of ZnS into CIS. The band gap of bulk ZnS (3.6 eV) is markedly higher than that of $CuInS_2$ (1.5 eV), and Zn^{2+} statistically replaces Cu^{+} and In^{3+}. Thus, it is reasonable to assume that the band gap of the $ZnSCuInS_2$ alloy is higher than that of CIS. This strategy for band gap tuning has been commonly used in ZnS–CdS and ZnSe–CdSe-alloyed nanostructures.[41]

The fluorescence emitting wavelength of the ZCIS cores were detected at λ_{ex} = 470 nm, as shown in Fig. 1B. It was observed that it is difficult to make Zn-free CIS NCs with a particle size that afforded an emission wavelength below 600 nm due to rapid particle growth. On the other hand, the addition of Zn in increasing amounts reduced the growth rate, as seen in the decreasing slope of the curves. The slower growth rate was beneficial for controlling the emission wavelength of the quantum dots. Furthermore, the addition of Zn facilitates the formation of QDs with a wider emission wavelength range. By changing the QD composition from Cu : In : Zn = 1 : 1 : 0.2 to Cu : In : Zn = 1 : 1 : 1, the minimum emission wavelength could be lowered from 580 to 530 nm.

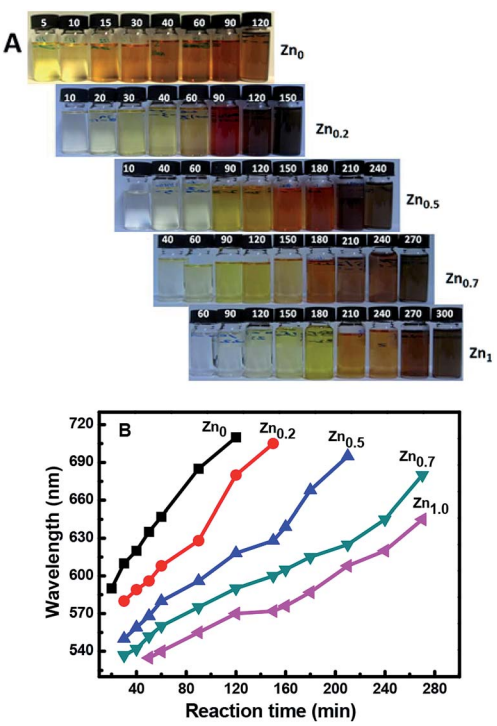

Fig. 1 Visible light photographs (A) and emission wavelengths (B) of the ZCIS core nanoparticles with different Zn ratios with increase in time at 230 °C.

Effect of the Cu : In ratio

Fig. 2 shows that the particle growth rate not only depends on the amount of added Zn but also on the Cu/In ratio. The QD growth rate at 30 min of reaction time is significantly higher at a Cu : In ratio of 1 : 4 compared to that at the Cu : In ratio of 1 : 1. This difference increased with increasing amounts of Zn. At a fixed reaction time/temperature and at a Zn content of 0.7, the fluorescent peak position at Cu/In = 1 : 1 is 537 nm, while at Cu/In = 1 : 2 and Cu/In = 1 : 4 it is 574 nm and 599 nm, respectively. This indicates that at a higher In content the nanoparticles grew faster and showed higher emission wavelengths. Thus, by adjusting the Zn content, the difference in the peak positions lessened more for the Cu/In = 1 : 4 samples than for the Cu/In = 1 : 1 samples. Therefore, adjusting the Zn content could produce QDs with an emission wavelength ranging from 585 nm to 635 nm (Cu/In = 1 : 4 with), 554 nm to 625 nm (Cu/In = 1 : 2), and 537 nm (or less) to 605 nm (Cu/In = 1 : 1). However, at the same reaction time, a higher In content could significantly improve the quantum yield (Fig. 2B); the emission intensity at Cu/In = 1 : 4 is much higher than that at a lower In content. These In-rich effects have also been reported for the CuInS system.[42] However, the QY at Cu/In = 1 : 1 can be improved by the subsequent deposition of the ZnS shell.

Effect of 1-dodecanethiol concentration

Fig. 3A shows that when the other reaction variables were held constant, such as the Zn/Cu/In ratio, the PL peak position of the resulting ZCIS NCs strongly depended on the thiol concentration with the increase in the reaction time. The dependence could be divided into two behaviors: when the amount of thiol was less than 1 mL, it barely had any effect on the PL peak position; however, when the amount of thiol was more than 1 mL, the PL peak shifted significantly towards shorter wavelengths. However, the concentration effect of 3 mL thiol is almost the same as that of 2 mL thiol. This could be ascribed to the composition variation in the presence of thiol contents over 1 mL.

Effect of reaction temperatures

Fig. 3B shows the dependence of PL wavelength on temperature during QD preparation. The shift of the PL peak towards longer wavelengths suggests an exponential increase in the growth rate of the QDs at reaction temperatures above 210 °C. Therefore, it becomes increasingly difficult to control the growth of QDs at high temperatures and the NCs precipitated within the reaction mixture at 250 °C in 1 h. Since 1-dodecanethiol acts both as a sulfur precursor and a stabilizing ligand during the reaction, its gradual decomposition at elevated temperatures destabilizes the colloids. However, due to the much slower growth rate and time consuming nature of QD formation with a weak PL emission at 210 °C, the reaction was better at 230 °C, where the growth was sufficiently controllable and yielded a comparably stronger PL emission band.

ZCIS/ZnS core/shell structure

Significant increase in the fluorescence emission intensity. Coating the ZCIS particles with ZnS shells showed a beneficial effect on the photoluminescence properties of the cores; more the shell layers, higher the emissions of the ZCIS/ZnS, as shown in Fig. 4A when the number of shell layers grows from one (a) to six (f). On the other hand, a blue-shift of the emission (Fig. 4A) and the absorption (Fig. 4B) band can be observed. Usually, most type I core–shell structures showed a red-shift of the

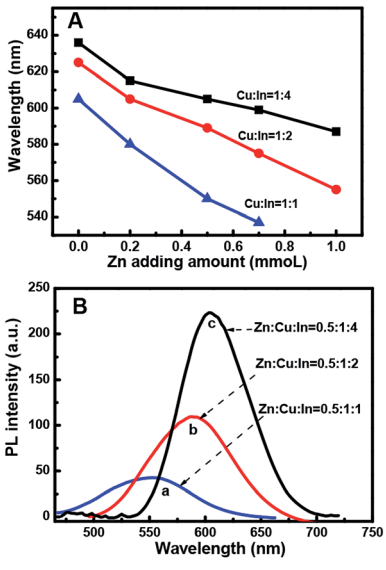

Fig. 2 (A) Emission wavelength of the ZnCuInS alloy nanoparticles with different zinc quantities and various Cu/In ratios at 230 °C, grown for 30 min with 0.5 mL 1-dodecanethiol. (B) PL emission spectra of the ZnCuInS alloy nanoparticles with various Cu/In ratios having Zn content of 0.5. All were grown for 30 min at 230 °C.

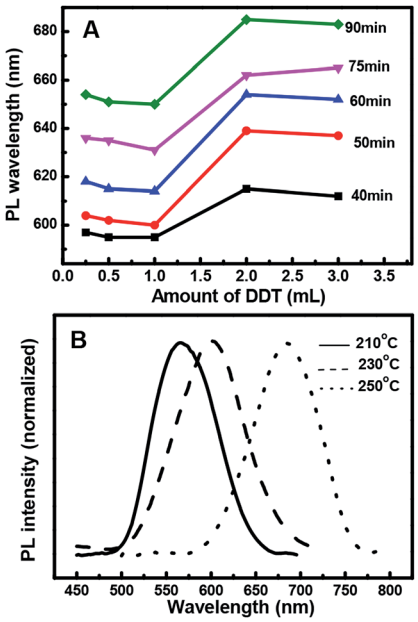

Fig. 3 (A) PL emission wavelength throughout the reaction process of the Zn-alloyed $CuInS_2$ nanoparticles with Zn/Cu/In = 0.2 : 1 : 2 with different 1-dodecanethiol amounts. (B) Effect of reaction temperature during QD preparation on their photoluminescence wavelength.

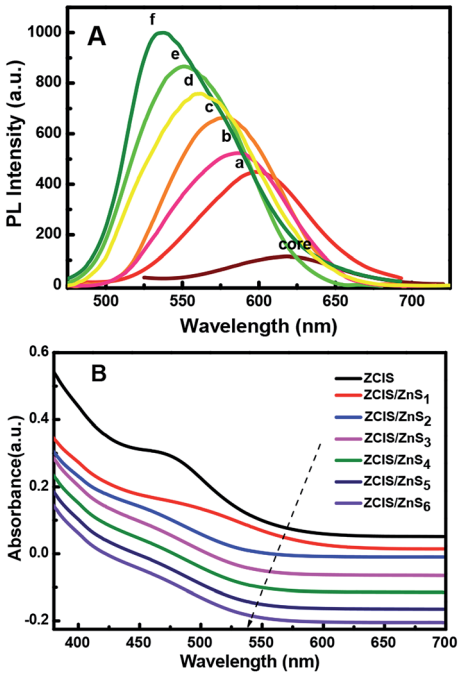

Fig. 4 PL emission spectra (A) of the resulting alloyed NCs with increasing number of ZnS shells deposited around the ZCIS core from one (a) to six (f) and their UV absorption (B).

absorption and emission bands after shell coating due to a slight delocalization of the charge carriers into the shell layer.[43] Such a blue-shift was reported in some other CIS–ZnS core–shell QDs cases.[44] Several different explanations for the blue-shift have been suggested, including surface reconstruction,[45] inter-diffusion of Zn atoms,[46] or etching of the core material.[47] The absorption spectra seen in Fig. 4B eliminate the possibility of Zn diffusion-associated blue-shift because the corresponding change in the band gap of the core/shell QDs was not observed. Surface reconstruction might be a cause of these findings, but it is difficult to claim without an appropriate theoretical or experimental understanding. Recently, it was found that cation exchange in the outer layer of the CIS nanocrystals explained the large blue-shift observed for the CIS–ZnS core–shell structures.[48]

Thus, the emission wavelength and QY of the resulting ZCIS/ZnS core/shell structure can be tuned by varying the band gap of the starting ZCIS core nanoparticles and *via* the batch-wise addition of ZnS for shell growth. Fig. 5A and B show that the emission wavelength of the ZCIS/ZnS core/shell NCs prepared from ZCIS core NCs with different Zn/Cu ratios have remarkable fluorescent emission brightness and cover most of the visible light region (from 527 nm to 700 nm).

Fig. 6 shows the wide-field TEM images of the $ZCIS_{620}$ core nanoparticles prepared from Zn/Cu/In = 0.2 : 1 : 2 at 230 °C in 1 h with an average size of 4 nm (Fig. 6A) as well as the corresponding $ZCIS/ZnS_{575}$ core/shell nanoparticles derived from the initial $ZCIS_{620}$ cores *via* the three-step growth of the ZnS shell at 230 °C with an average size of 10 nm (Fig. 6D). The AFM measurements also confirmed the change in size during the shell growth, as shown in Fig. 6B and C. The diameter of the

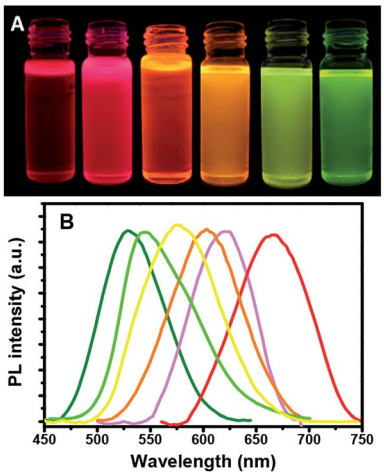

Fig. 5 Normalized PL spectra (λ_{ex} = 365 nm) of ZCIS/ZnS core/shell NCs obtained from ZCIS core with different Zn/Cu ratios (A) and the representative emission colors of NC dispersion in toluene under the radiation of a UV lamp (B).

$ZCIS_{620}$ core particles is about 3 ± 0.4 nm, while the corresponding $ZCIS/ZnS_{575}$ particles displayed a size of about 11 ± 0.6 nm. Hence, the blue-shift in the emission wavelength was not caused by smaller size and the shell growth induced a size enhancement, leading to a blue-shift instead of a red-shift.

Ionic liquid-soluble NCs *via* ligand exchange. Ligand exchange endows NCs with wide application potential, such as co-solvation with other polymers or provides covalent bonding for reaction with polymers. Herein, we could successfully cause thiol-ligand exchange by 3-mercaptopropyl-trimethoxysilane with the help of the ionic liquid 1-hexyl-3-methylimidazolium chloride as the solvent. It should be mentioned that we tried other ionic liquids, such as 1-ethyl-3-methylimidazolium chloride and 1-butyl-3-methylimidazolium chloride, but only the long chain 1-hexyl-3-methylimidazolium chloride could successfully aid in the ligand exchange from DDT to 3-mercaptopropyl-trimethoxysilane for the ZCIS/ZnS nanoparticles and transfer the groups from toluene to the ionic

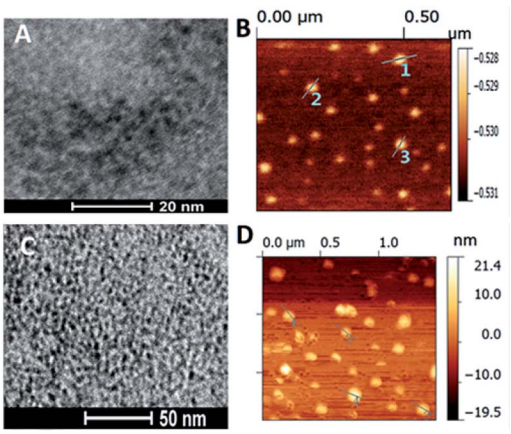

Fig. 6 Wide-field TEM and AFM images of $ZCIS_{620}$ (A and B). Zn/Cu/In = 0.2 : 1 : 1 in 1 h at 230 °C and its corresponding $ZCIS/ZnS_{575}$ (C and D) after 3 batches of Zn shell growth on the core.

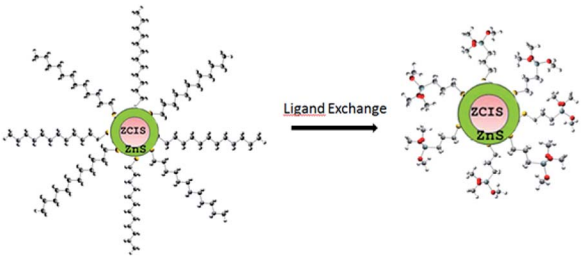

Fig. 7 ZCIS/ZnS capped with 1-dodecanethiol and ligand exchange with (3-mercaptopropyl)trimethoxysilane.

liquid 1-hexyl-3-methylimidazolium chloride. This solved the traditional problem of difficult DDT ligand exchange. The strong interactions between the mercapto group of MPTMS was the key factor in the successful ligand exchange of 1-dodecanethiol with MPTMS, as illustrated in Fig. 7. These nanoparticles can be converted from hydrophobic to hydrophilic *via* ligand exchange, thus rendering them readily dispersible in ionic liquids, as shown in Fig. 8. The ionic liquid-soluble ZCIS/ZnS NCs could retain up to 70% of the luminescent intensity of the original oleophilic NCs (Fig. 8A). Moreover, the fluorescent emission peak with a narrow fluorescent region red-shifts by about 10 nm, indicating that the red-shift was induced not by aggregation but rather by the changing environment. Fig. 8B shows luminescence in both toluene and ionic liquids under a UV lamp. The high luminescence of ZCIS/ZnS in the ionic liquid could be retained for several months without any observable quenching. This high PL stability and compatibility of the ionic liquid-soluble QDs is of special interest in the preparation of composite materials with polymers.

The ligand exchange behavior was further analyzed *via* GC-MS. The standard calibration curve of 1-dodecanethiol was obtained using Br-decane as the internal standard. The equation $y = 0.4929x$ describes the ligand exchange behavior. Herein, different amounts of QDs were used for ligand exchange and the corresponding ligand 1-dodecanethiol remained in

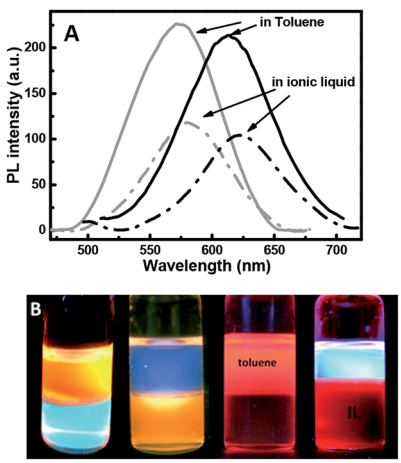

Fig. 8 Fluorescent spectra of ZCIS/ZnS core–shell samples before and after ligand exchange that stayed in toluene and ionic liquid (A) and the corresponding luminescent photographs under a UV lamp (B).

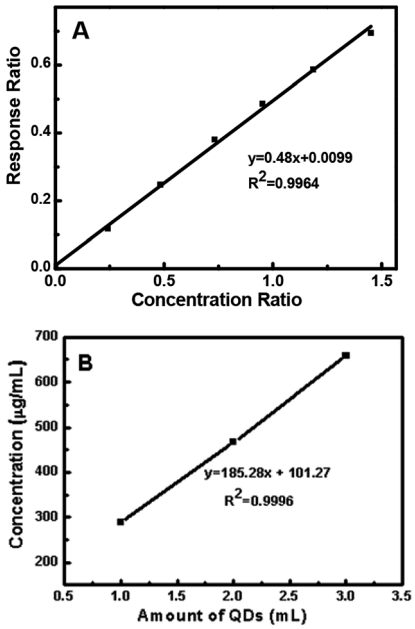

Fig. 9 GC-MS standard curve for 1-dodecanethiol (A) and the relationship between the QD concentration and responses for 1-dodecanethiol (B).

toluene after ligand exchange. This was found to follow the trend, as shown in Fig. 9. The remaining 1-dodecanethiol in the three samples showed a linear increase with increasing amounts of 1-mercapto-*n*-dodecane-capped QDs. According to the equation $y = 185.28x + 101$ (ref. 49) (y is the estimated concentration of the remaining 1-dodecanethiol in toluene (μg mL^{-1})), 1-dodecanethiol was successfully exchanged by (3-mercaptopropyl)trimethoxysilane. In addition, the linear trend implies that the exchange percentage of 1-dodecanethiol was the same every time.

Conclusions

ZCIS-alloyed NCs were prepared *via* a sulfur injection-free approach in the non-coordinating solvent octadecene in the presence of 1-dodecanethiol using copper iodide and indium and zinc acetates as the precursors. The band gap of the ZCIS-alloyed NCs can be conveniently tuned by adjusting the experimental variables, such as the Zn content, Cu : In ratio, dodecanethiol concentration, and reaction temperature. With the deposition of ZnS shells around the ZCIS cores, the PL QY increased substantially to a maximum value of 35%, while the emission wavelength underwent a blue-shift and could be tuned from 518 nm to 810 nm. The ionic liquid-soluble ZCIS/ZnS NCs obtained through ligand exchange could preserve the high PL emission efficiency, which was confirmed by GC-MS and PL measurements. Thus these novel, toxic-free fluorescent nanoparticles are promising in composite applications.

Conflicts of interest

There are no conflicts to declare.

Acknowledgements

The authors would like to thank the internal cooperation from the University of Natural Resources and Life Sciences Vienna: Jose Toca-Herrera, David Schuster, Jaqueline Friedmann, Haizheng Zhong (School of Materials Science & Engineering, Beijing Institute of Technology). The financial supports from the National Natural Science Foundation of China (51603059), Fundamental Research Fund for the Central Universities of China (106-4115100027), China Postdoctoral Foundation, and AnHui Provence Postdoctoral Foundation are gratefully acknowledged. The Christian Doppler Laboratory ''Advanced cellulose chemistry and analytics'' is thankfully acknowledged.

References

1 H. Abdullah and D. H. Kuo, *ACS Appl. Mater. Interfaces*, 2015, **7**, 26941–26951.
2 B. Clemens, X. Chen, R. Narayanan and M. El-Sayed, *Chem. Rev.*, 2005, **105**, 1025–1029.
3 P. Alivisatos, *Nat. Biotechnol.*, 2004, **22**, 47–52.
4 B. K. Chen, H. Z. Zhong, W. Q. Zhang, *et al.*, *Adv. Funct. Mater.*, 2012, **22**, 2081–2088.
5 T. Tomai, Y. Yasui and S. Watanabe, *J. Supercrit. Fluids*, 2016, **120**, 448–452.
6 E. Belas, Uxa and R. Grill, *J. Appl. Phys.*, 2014, **116**, 103521.
7 Y. Chen, X. Guo and C. Xie, *Int. J. Hydrogen Energy*, 2018, **43**, 13911–13920.
8 D. Pan, D. Weng, X. Wang, Q. Xiao, W. Chen, C. Xu, *et al.*, *Chem. Commun.*, 2009, **28**, 4221–4223.
9 M. Kruszynska, H. Borchert, J. Parisi, *et al.*, *J. Am. Chem. Soc.*, 2010, **132**, 15976–15986.
10 X. Tang, W. Cheng, E. S. G. Choo, *et al.*, *Chem. Commun.*, 2011, **47**, 5217–5219.
11 X. Wang, D. Pan, D. Weng, C.-Y. Low, L. Rice, J. Han and Y. Lu, *J. Phys. Chem. C*, 2010, **114**, 13406–13413.
12 W.-S. Song, J.-H. Kim, J.-H. Lee, H.-S. Lee, Y. R. Do and H. Yang, *J. Mater. Chem.*, 2012, **22**, 21901–21908.
13 Y.-H. Wang, X. Zhang, N. Bao, B. Lin and A. Gupta, *J. Am. Chem. Soc.*, 2011, **133**, 11072–11075.
14 Q. Liu, Z. Zhao, Y. Lin, P. Guo, S. Li, D. Pan and X. Ji, *Chem. Commun.*, 2011, **47**, 964–966.
15 W. Zhang and X. Zhong, *Inorg. Chem.*, 2011, **50**, 4065–4072.
16 J. Feng, M. Sun, F. Yang and X. Yang, *Chem. Commun.*, 2011, **47**, 6422–6424.
17 X. Wang, D. Pan, D. Weng, C.-Y. Low, L. Rice, J. Han and Y. Lu, *J. Phys. Chem. C*, 2010, **114**, 13406–13413.
18 H. J. Pan, C. W. Lai and S. W. Chou, *Mater. Express*, 2012, **2**, 224–232.
19 D. Pan, D. Weng, X. Wang, Q. Xiao, W. Chen, C. Xu, Z. Yang and Y. Lu, *Chem. Commun.*, 2009, **40**, 4221–4223.
20 H. Nakamura, W. Kato, M. Uehara, K. Nose, T. Omata, S. Otsuka-Yao-Matsuo, M. Miyazaki and H. Maeda, *Chem. Mater.*, 2006, **18**, 3330–3335.
21 L. De Trizio, M. Prato, A. Genovese, A. Casu, M. Povia, R. Simonutti, M. J. P. Alcocer, C. D. Andrea, F. Tassone and L. Manna, *Chem. Mater.*, 2012, **24**, 2400–2406.
22 E. J. Tyrrell and S. Tomic, *J. Phys. Chem. C*, 2015, **119**, 12720–21273.
23 N. Radychev, D. Scheunemann, M. Kruszynska, K. Frevert, R. Miranti, *et al.*, *Org. Electron.*, 2012, **13**, 3154–3164.
24 Z. Bai, W. Ji, D. Han, *et al.*, *Chem. Mater.*, 2016, **28**, 1085–1091.
25 M. Booth, A. Brown, S. Evans and K. Critchley, *Chem. Mater.*, 2012, **24**, 2064–2070.
26 W. Guo, N. Chen, Y. Tu, C. Dong, B. Zhang, C. Hu and J. Chang, *Theranostics*, 2013, **3**, 99–108.
27 L. Li, T. J. T. Daou, I. Texier, T. K. Chi, T. T. Kim Chi, N. Q. Liem and P. Reiss, *Chem. Mater.*, 2009, **21**, 2422–2429.
28 K. Yu, P. Ng, J. Ouyang, M. Badruz Zaman, A. Abulrob, T. N. Baral, D. Fetehi, Z. J. Jakubek, D. Kingston, X. Wu, X. Liu, C. Hebert, D. M. Leek and D. M. Whitfield, *ACS Appl. Mater. Interfaces*, 2013, **5**, 2870–2880.
29 J. Feng, M. Sun, F. Yang and X. Yang, *Chem. Commun.*, 2011, **47**, 6422–6424.
30 C. C. Chang, P. H. Chen and C. M. Chang, *J. Sol-Gel Sci. Technol.*, 2008, **47**, 268–273.
31 S. S. Kim, J. E. Park and J. Lee, *J. Appl. Polym. Sci.*, 2011, **119**, 2261–2267.
32 A. S. Amarasekara and D. G. Reyes, *Renewable Energy*, 2019, **136**, 352–357.
33 J. Wu, J. Zhang, H. Zhang, J. He, Q. Ren and M. Guo, *Biomacromolecules*, 2004, **5**, 266–268.
34 R. P. Swatloski, S. K. Spear, J. D. Holbery, *et al.*, *J. Am. Chem. Soc.*, 2002, **124**, 4974–4975.
35 G. Fan, C. Liao, T. Fang, M. Wang and G. Song, *Fuel Process. Technol.*, 2013, **116**, 142–148.
36 J. Hulsbosch, D. E. D. Vos, K. Binnemans, *et al.*, *RSC Adv.*, 2016, **6**, 4053–4062.
37 M. M. Jaworska and A. Gorak, *Mater. Lett.*, 2016, **164**, 341–343.
38 I. Bushra, M. Nawshad, R. Abdur, *et al.*, *Int. J. Polym. Mater. Polym. Biomater.*, 2019, **68**, 590–596.
39 J. Li, B. Kempken, V. Dzhagan, *et al.*, *CrystEngComm*, 2015, **17**, 5634–5643.
40 D.-E. Nam, W.-S. Song and H. Yang, *J. Colloid Interface Sci.*, 2011, **361**, 491–496.
41 H. Zhong, Y. Zhou, M. Ye, Y. He, J. Ye, C. He, C. Yang and Y. Li, *Chem. Mater.*, 2008, **20**, 6434–6443.
42 S. L. Castro, S. G. Bailey, R. P. Raffaelle, K. K. Banger and A. F. Hepp, *J. Phys. Chem. B*, 2004, **108**, 12429–12435.
43 M. Booth, A. Brown, S. Evans and K. Critchley, *Chem. Mater.*, 2012, **24**, 2064–2070.
44 J. Park and S.-W. Kim, *J. Mater. Chem.*, 2011, **21**, 3745–3750.
45 L. Li, T. J. Daou, I. Texier, T. K. K. Chi, N. Q. Liem and P. Reiss, *Chem. Mater.*, 2009, **21**, 2422–2429.
46 T. Pons, E. Pic, N. Lequeux, E. Cassette, L. Bezdetnaya, F. Guillemin, F. Marchal and B. Dubertret, *ACS Nano*, 2010, **4**, 2531–2538.
47 L. Li, A. Pandey, D. J. Werder, B. P. Khanal, *et al.*, *J. Am. Chem. Soc.*, 2011, **133**, 1176–1179.
48 J. Park and S.-W. Kim, *J. Mater. Chem.*, 2011, **21**, 3745–3750.
49 H. Y. Park, I. Ryu and J. Kim, *J. Phys. Chem. C*, 2014, **118**, 17374–17382.

